KINGDOM OF SAUDI ARABIA
Northern Border University (NBU)
Journal of the North for Basic & Applied Sciences(JNBAS)
p - ISSN : 1658 -7022 / **e-ISSN:** 1658 - 7014
www.nbu.edu.sa
s.journal@nbu.edu.sa

Analytical Traveling-Wave Solutions of the Conformable Fractional (2+1)-Dimensional Zakharov–Kuznetsov Equation via the Unified Method

Elzain A. E. Gumma
Department of Mathematics, College of Science, Northern Border University, Arar, Saudi Arabia.

(**Received:** 11th November 2025; **Accepted:** 20th December 2025)

Abstract
This study investigates the time conformable fractional (2+1)-dimensional Zakharov–Kuznetsov (ZK) equation using the Unified Method (UM) to obtain analytical traveling-wave solutions. The derived solutions include hyperbolic, trigonometric, and rational function forms that describe different nonlinear wave behaviors. Graphical analyses are carried out for different fractional orders to examine how the fractional parameter influences wave configuration and amplitude. The findings indicate that a reduction in the fractional order causes the nonlinear wave profiles to transition gradually from localized soliton patterns to smoother, dissipative structures. This confirms the UM is a powerful, systematic, and efficient analytical tool for solving a wide class of fractional nonlinear partial differential equations.

Keywords: Unified method; nonlinear fractional partial differential equation; fractional derivatives; traveling-wave solutions.

(*) **Corresponding Author**:
By Elzain A. E. Gumma
Department of Mathematics, College of Science, Northern Border University, Arar, Saudi Arabia.

DOI: 10.12816/0062496

1. Introduction

Nonlinear partial differential equations (NLPDEs) are fundamental to modeling and interpreting complex behaviors in physical, biological, and engineering systems. They have found extensive applications in fluid mechanics, material sciences, environmental modeling, biomedical engineering, physics-informed machine learning, and quantum research [1–6].

Various analytical approaches have been proposed for obtaining exact solutions of NLPDEs, including the Jacobi elliptic function expansion method [7], (G′/G)-expansion [8], the Tanh–Sech method [9], and modified (w/g)-expansion methods [10]. In this work, the unified method (UM) is employed to derive analytical solutions of the time-fractional (2+1)-dimensional ZK equation. Compared with the aforementioned methods, the UM provides greater flexibility with fewer restrictive assumptions and, unlike integrability-dependent techniques, is well suited for fractional, non-integrable, and multidimensional nonlinear equations. The ZK equation is a multidimensional generalization of the well-known Korteweg–de Vries (KdV) equation, which models the evolution of weakly nonlinear ion-acoustic waves in a magnetized plasma.

As defined in [4], the (2+1)-dimensional ZK equation is mathematically expressed as:

$$\varphi_t + a\varphi\, {\varphi^p}_x + \mathrm{b}({\varphi^q}_{xx} + {\varphi^r}_{xy})_x = 0. \quad (1)$$

where $a, b \in \mathbb{R}, p, q, r \in \mathbb{Z}, x$ and y are spatial coordinates and t the time. The nonlinear parameter values (p, q, r) lead to more complex wave structures, such as amplitude modulation, wave steepening, and enhanced nonlinear interactions, which can be addressed by the same analytical framework. The ZK equation arises from the dynamics of ion-acoustic waves from the dynamics of ion-acoustics waves in a magnetized plasma. The ZK equation has significant applications in several areas of physics including, astrophysics, fluid dynamics and nonlinear optics [11].

Although several fractional derivatives exist, this study employs the conformable fractional derivative (CFD) for the fractional (2+1)-dimensional ZK equation because it avoids nonlocal integral kernels while retaining essential classical calculus properties such as linearity and the product and chain rules. Unlike Riemann–Liouville [12], beta [13] and Caputo [14] fractional derivatives, the CFD simplifies analytical and symbolic computations, allowing standard techniques like traveling-wave reductions to be applied directly. At the same time, it captures local fractional dynamics and weak memory effects while remaining closely connected to classical models. The fractional (2+1)-dimensional ZK equation is

$$\mathbb{D}_t^\alpha \varphi + a\varphi\varphi_x + \mathrm{b}(\varphi_{xx} + \varphi_{xy})_x = 0, \;\; 0 < \alpha \leq 1. \quad (2)$$

In this expression, $\mathbb{D}_t^\alpha$ in CFD indicates the conformable fractional derivative of order α with respect to t. By adjusting the fractional order α, a broad range of wave propagation phenomena between purely local (classical).

As introduced in [15], the CFD of order with respect to the independent variable can be formulated as follows:

$$\mathbb{D}^\alpha \varphi(t) = \lim_{\delta \to 0} \frac{\varphi(t+\delta t^{1-\alpha}) - \varphi(t)}{\delta}, 0 < \alpha \leq 1.$$

$$\varphi^{(\alpha)}(0) = \lim_{\delta \to 0^+} \varphi^{(\alpha)}(t).$$

According to [15, 16], the CFD retains the basic properties of the classical derivative, supports analytical and numerical solution procedures for fractional differential equations. In this work, the UM is employed to derive exact solutions of the conformable time fractional ZK equation.

The UM is a versatile analytical technique that yields exact closed-form solutions for nonlinear and fractional partial differential equations without relying on small parameters [17-20].

The primary goal of this work is to verify the capability and efficiency of the applied method in addressing the fractional ZK equation. Although several studies have examined the nonlinear ZK equation using various analytical techniques, the unified method has not been wildly applied to its fractional counterpart [11,21]. The originality of this study stems from employing the unified method to obtain exact analytical solutions for the fractional ZK equation, which has received limited attention in previous research. The remainder of this paper is structured as follows: Section 2 outlines the unified method. Section 3 demonstrates its implementation for the fractional ZK equation, Section 4 displays and analyzes the graphical results, Section 5 discussed the stability of the unified method and Section 6 summarizes the key conclusions of the study.

2. Description of the unified method

The procedural steps of the method can be summarized as follows [18]:

Step 1: Consider a NLFPDE of the form:

$$F(\varphi, \mathbb{D}_t^\alpha \varphi, \mathbb{D}_x^\alpha \varphi, \varphi_x, \varphi_y, \varphi_{xx}, \varphi_{yy}, \ldots) = 0. \quad (3)$$

To determine the analytical solutions of Eq. (3), the following traveling-wave transformation is introduced,

$$\varphi(x, y, t) = \varphi(\zeta), \zeta = x + y - ct^\alpha/\alpha. \quad (4)$$

Eq. (3) is reduced to an ODE:

$$F(\varphi, \varphi', \varphi'', \varphi''', \ldots) = 0, \quad (5)$$

where $\varphi' = \frac{d\varphi}{d\zeta}$.

Step 2: The solution Eq. (5) is assumed to be of the form:

$$\varphi(\zeta) = a_0 + \sum_{i=1}^{N}[a_j\Omega^i + b_j\Omega^{-i}], \tag{6}$$

where $\Omega = \Omega(\zeta)$ satisfies the Riccati equation

$$\Omega' = \tau + \Omega^2(\zeta), \tag{7}$$

where τ is a constant. The positive integer N is determined by balancing the highest-order derivative terms with the highest-degree nonlinear terms in Eq. (5). Moreover y, a_0 , a_j, b_j $(1 \le i \le N)$ represent unknown coefficients to be determined.

Step 3: Substituting Eqs. (6) and (7) into Eq. (5) and equating the coefficients of identical powers of to zero, a system of algebraic equations is obtained. This system is solved symbolically using Maple to compute the parameters a_0, a_i, b_i and τ. The obtained parameters, along with the general form of Eq. (6), are then employed to construct the exact solutions of Eq. (3).

The general solutions of Eq. (7) can be classified into three distinct families as follows:

Family 1. If $\tau < 0$, the corresponding solutions are expressed as

$$\Omega(\zeta) = \begin{cases} \Omega_1 = \dfrac{\sqrt{-(\rho^2+\nu^2)\tau} - \rho\sqrt{-\tau}\cosh\left(2\sqrt{-\tau}(\zeta+\zeta_0)\right)}{\rho\sinh\left(2\sqrt{-\tau}(\zeta+\zeta_0)\right)+\nu} \\ \Omega_2 = \dfrac{-\sqrt{-(\rho^2+\nu^2)\tau} - \rho\sqrt{-\tau}\cosh\left(2\sqrt{-\tau}(\zeta+\zeta_0)\right)}{\rho\sinh\left(2\sqrt{-\tau}(\zeta+\zeta_0)\right)+\nu} \\ \Omega_3 = \sqrt{-\tau} + \dfrac{-2\rho\sqrt{-\tau}}{\rho+\cosh\left(2\sqrt{-\tau}(\zeta+\zeta_0)\right)-\sinh\left(2\sqrt{-\tau}(\zeta+\zeta_0)\right)} \\ \Omega_4 = -\sqrt{-\tau} + \dfrac{2\rho\sqrt{-\tau}}{\rho+\cosh\left(2\sqrt{-\tau}(\zeta+\zeta_0)\right)+\sinh\left(2\sqrt{-\tau}(\zeta+\zeta_0)\right)} \end{cases} \tag{8}$$

Family 2. If $\tau > 0$, the solutions are

$$\Omega(\zeta) = \begin{cases} \Omega_5 = \dfrac{\sqrt{(\rho^2-\nu^2)\tau} - \rho\sqrt{\tau}\cos\left(2\sqrt{\tau}(\zeta+\zeta_0)\right)}{\rho\sin\left(2\sqrt{\tau}(\zeta+\zeta_0)\right)+\nu} \\ \Omega_6 = \dfrac{-\sqrt{(\rho^2-\nu^2)\tau} - \rho\sqrt{\tau}\cos\left(2\sqrt{\tau}(\zeta+\zeta_0)\right)}{\rho\sin\left(2\sqrt{\tau}(\zeta+\zeta_0)\right)+\nu} \\ \Omega_7 = i\sqrt{\tau} + \dfrac{-2\rho i\sqrt{\tau}}{\rho+\cos\left(2\sqrt{\tau}(\zeta+\zeta_0)\right)-i\sin\left(2\sqrt{\tau}(\zeta+\zeta_0)\right)} \\ \Omega_8 = -i\sqrt{\tau} + \dfrac{2\rho i\sqrt{\tau}}{\rho+\cos\left(2\sqrt{\tau}(\zeta+\zeta_0)\right)+i\sin\left(2\sqrt{\tau}(\zeta+\zeta_0)\right)} \end{cases} \tag{9}$$

Family 3. If $\tau = 0$, the solution is

$$\Omega(\zeta) = -\frac{1}{\zeta+\zeta_0},$$

where $\rho \neq 0$ and $\nu, \zeta_0 \in \mathbb{R}$. , (10)

3. Application of the unified method

This section applies the unified method to obtain analytical solutions of Eq. (2). By employing the traveling wave transformation given in Eq. (4), Eq. (2) with p = q = r = 1 reduces to

$$-c\varphi' + a\varphi\varphi' + 2b\varphi''' = 0. \tag{11}$$

Integrating Eq. (11) and setting the constant of integration to zero to obtain

$$-c\varphi + \frac{a}{2}\varphi^2 + 2b\varphi'' = 0. \tag{12}$$

By balancing highest-order derivative term with the nonlinear term , yields Therefore, the solution of Eq. (12) can be represented as

$$\varphi(\zeta) = a_0 + a_1\Omega + a_2\Omega^2 + b_1\Omega^{-1} + b_2\Omega^{-2}. \tag{13}$$

When Eqs. (13) and (7) are substituted into Eq. (5), and the coefficients of the same powers of are equated to zero, a system of algebraic equations emerges. This system is subsequently solved symbolically using Maple, resulting in the following sets of parameters:

Set 1: $a_0 = 8\tau b \pm \frac{\sqrt{64b^2\tau^2-2a}}{2}, a_1 = 0, a_2 = 12b,\ b_1 = 0,\ b_2 = 0,$

$c = \pm\sqrt{64b^2\tau^2 - 2a}.$

Set 2: $a_0 = 8\tau b \pm \frac{\sqrt{1024b^2\tau^2-2a}}{2}, a_1 = 0, a_2 = 12b,\ b_1 = 0,\ b_2 = 12b\,\tau^2,$

$c = \pm\sqrt{1024b^2\tau^2 - 2a}.$

Set 3: $a_0 = 8\tau b \pm \frac{\sqrt{64b^2\tau^2-2a}}{2}, a_1 = 0, a_2 = 0,\ b_1 = 0,\ b_2 = 12b\,\tau^2,$

$c = \pm\sqrt{64b^2\tau^2 - 2a}.$

Based on the previously obtained parameter sets corresponding to Families 1–3, the exact hyperbolic, trigonometric, and rational forms of the solutions to the conformable time-fractional ZK equation are derived as follows:

Family 1: For the case $\tau < 0$.

For Set (1), the Eq. (13) yields the following solutions

$$\varphi_1(x,y,t) = 8\tau b \pm \frac{\sqrt{64b^2\tau^2-2a}}{2} \pm 12b\left(\frac{\sqrt{-(\rho^2+\nu^2)} - \beta\sqrt{-\tau}\cosh\left(2\sqrt{-\tau}\left(x+y\pm\frac{\sqrt{64b^2\tau^2-2at^\alpha}}{\alpha}+\zeta_0\right)\right)}{\rho\sinh\left(2\sqrt{-\tau}(\zeta+\zeta_0)\right)+\nu}\right)^2,$$

$$\varphi_2(x,y,t) = 8\tau b \pm \frac{\sqrt{64b^2\tau^2-2a}}{2} \pm 12b\left(\sqrt{-\tau} + \frac{-2\rho\sqrt{-\tau}}{\rho+\cosh\left(2\sqrt{-\tau}(\zeta+\zeta_0)\right)-\sinh\left(2\sqrt{-\tau}(\zeta+\zeta_0)\right)}\right)^2,$$

$$\varphi_3(x,y,t) = 8\tau b \pm \frac{\sqrt{64b^2\tau^2-2a}}{2} \pm 12b\left(-\sqrt{-\tau} + \frac{-2\rho\sqrt{-\tau}}{\rho+\cosh\left(2\sqrt{-\tau}(\zeta+\zeta_0)\right)+\sinh\left(2\sqrt{-\tau}(\zeta+\zeta_0)\right)}\right)^2,$$

Where $\zeta = x + y \pm \frac{\sqrt{64b^2\tau^2-2at^\alpha}}{\alpha}$.

In Set (2): Equation (13) yields the following solutions.

$$\varphi_4(x,y,t) = 8\tau b \pm \frac{\sqrt{1024b^2\tau^2-2a}}{2} \pm 12b\left(\frac{\sqrt{-(\rho^2+\nu^2)\tau} - \rho\sqrt{-\tau}\cosh\left(2\sqrt{-\tau}(\zeta+\zeta_0)\right)}{\rho\sinh\left(2\sqrt{-\tau}(\zeta+\zeta_0)\right)+\nu}\right)^2 \pm 12b\,\tau^2\left(\frac{\sqrt{-(\rho^2+\nu^2)\tau} - \rho\sqrt{-\tau}\cosh\left(2\sqrt{-\tau}(\zeta+\zeta_0)\right)}{\rho\sinh\left(2\sqrt{-\tau}(\zeta+\zeta_0)\right)+\nu}\right)^{-2},$$

$$\varphi_5(x,y,t) = 8\tau b \pm \frac{\sqrt{1024b^2\tau^2-2a}}{2} \pm 12b\left(\sqrt{-\tau} + \frac{-2\rho\sqrt{-\tau}}{\rho+\cosh\left(2\sqrt{-\tau}(\zeta+\zeta_0)\right)-\sinh\left(2\sqrt{-\tau}(\zeta+\zeta_0)\right)}\right)^2 \pm 12b\,\tau^2\left(\sqrt{-\tau} + \frac{-2\rho\sqrt{-\tau}}{\rho+\cosh\left(2\sqrt{-\tau}(\zeta+\zeta_0)\right)-\sinh\left(2\sqrt{-\tau}(\zeta+\zeta_0)\right)}\right)^{-2},$$

$$\varphi_6(x,y,t) = 8\tau b \pm \frac{\sqrt{1024b^2\tau^2-2a}}{2} \pm 12b\left(\sqrt{-\tau} + \frac{-2\rho\sqrt{-\tau}}{\rho+\cosh\left(2\sqrt{-\tau}(\zeta+\zeta_0)\right)+\sinh\left(2\sqrt{-\tau}(\zeta+\zeta_0)\right)}\right)^2 \pm 12b\,\tau^2\left(\sqrt{-\tau} + \frac{-2\rho\sqrt{-\tau}}{\rho+\cosh\left(2\sqrt{-\tau}(\zeta+\zeta_0)\right)-\sinh\left(2\sqrt{-\tau}(\zeta+\zeta_0)\right)}\right)^{-2},$$

$\zeta = x + y \pm \frac{\sqrt{1024b^2\tau^2 - 2at^\alpha}}{\alpha}.$

In **Set (3)**, Eq. (13) provides the corresponding solutions.

$$\varphi_7(x,y,t) = 8\tau b \pm \frac{\sqrt{64b^2\tau^2-2a}}{2} \pm 12b\,\tau^2\left(\frac{\sqrt{-(\rho^2+\nu^2)\tau}-\rho\sqrt{-\tau}\cosh\left(2\sqrt{-\tau}(\zeta+\zeta_0)\right)}{\rho\sinh\left(2\sqrt{-\tau}(\zeta+\zeta_0)\right)+\nu}\right)^{-2},$$

$$\varphi_8(x,y,t) = 8\tau b \pm \frac{\sqrt{64b^2\tau^2-2a}}{2} \pm 12b\left(\sqrt{-\tau}+\frac{-2\rho\sqrt{\tau}}{\rho+\cosh\left(2\sqrt{-\tau}(\zeta+\zeta_0)\right)-\sinh\left(2\sqrt{-\tau}(\zeta+\zeta_0)\right)}\right)^{-2},$$

$$\varphi_9(x,y,t) = 8\tau b \pm \frac{\sqrt{64b^2\tau^2-2a}}{2} + 12b\left(-\sqrt{-\tau}+\frac{-2\rho\sqrt{\tau}}{\rho+cosh\left(2\sqrt{-\tau}(\zeta+\zeta_0)\right)+sinh\left(2\sqrt{-\tau}(\zeta+\zeta_0)\right)}\right)^{-2},$$

$$\zeta = x + y \pm \frac{\sqrt{64b^2\tau^2-2a}\,t^\alpha}{\alpha}.$$

Family 2: For the case $\tau > 0$.

For Set (1), the resulting solutions can be directly obtained from Eq. (13).

$$\varphi_{10}(x,y,t) = 8\tau b \pm \frac{\sqrt{64b^2\tau^2-2a}}{2} \pm 12b\left(\frac{\sqrt{(\rho^2-\nu^2)\tau}-\rho\sqrt{\tau}\cos\left(2\sqrt{\tau}(\zeta+\zeta_0)\right)}{\rho\sin\left(2\sqrt{\tau}(\zeta+\zeta_0)\right)+\nu}\right)^{2},$$

$$\varphi_{11}(x,y,t) = 8\tau b \pm \frac{\sqrt{64b^2\tau^2-2a}}{2} \pm 12b\left(i\sqrt{\tau}+\frac{-2\rho i\sqrt{\tau}}{\rho+\cos\left(2\sqrt{\tau}(\zeta+\zeta_0)\right)-i\sin\left(2\sqrt{\tau}(\zeta+\zeta_0)\right)}\right)^{2},$$

$$\varphi_{12}(x,y,t) = 8\tau b \pm \frac{\sqrt{64b^2\tau^2-2a}}{2} \pm 12b\left(-i\sqrt{\tau}+\frac{2\rho i\sqrt{\tau}}{\rho+\cos\left(2\sqrt{\tau}(\zeta+\zeta_0)\right)+i\sin\left(2\sqrt{\tau}(\zeta+\zeta_0)\right)}\right)^{2},$$

where $\zeta = x + y \pm \frac{\sqrt{64b^2\tau^2-2a}t^\alpha}{\alpha}$.

Under **Set (2)**, the analytical solutions are derived from Eq. (13) as follows.

Considering to **Set (3)**, Equation (13) produces the following set of solutions.

$$\varphi_{16}(x,y,t) = 8\tau b \pm \frac{\sqrt{64b^2\tau^2-2a}}{2} \pm 12b\left(\frac{\sqrt{(\rho^2-\nu^2)\tau}-\rho\sqrt{\tau}\cos\left(2\sqrt{\tau}(\zeta+\zeta_0)\right)}{\rho\sin\left(2\sqrt{\tau}(\zeta+\zeta_0)\right)+\nu}\right)^{2},$$

$$\varphi_{17}(x,y,t) = 8\tau b \pm \frac{\sqrt{64b^2\tau^2-2a}}{2} \pm 12b\,\tau^2\left(i\sqrt{\tau}+\frac{-2\rho i\sqrt{\tau}}{\rho+\cos\left(2\sqrt{\tau}(\zeta+\zeta_0)\right)-i\sin\left(2\sqrt{\tau}(\zeta+\zeta_0)\right)}\right)^{-2},$$

$$\varphi_{18}(x,y,t) = 8\tau b \pm \frac{\sqrt{64b^2\tau^2-2a}}{2} \pm 12b\left(-i\sqrt{\tau}+\frac{2\rho i\sqrt{\tau}}{\rho+\cos\left(2\sqrt{\tau}(\zeta+\zeta_0)\right)+i\sin\left(2\sqrt{\tau}(\zeta+\zeta_0)\right)}\right)^{-2},$$

where $\zeta = x + y \pm \frac{\sqrt{64b^2\tau^2-2a}t^\alpha}{\alpha}$.

Family 3: For the case $\tau = 0$.

Sets (1–3): The corresponding solutions are derived from Eq. (13), respectively.

$$\varphi_{19}(x,y,t) = \frac{\sqrt{-2a}}{2} + 12b\left(-\frac{1}{\zeta+\zeta_0}\right)^2,$$

$$\varphi_{20}(x,y,t) = \pm\frac{\sqrt{-2a}}{2} + 12b\left(-\frac{1}{\zeta+\zeta_0}\right)^2,$$

$\varphi_{21}(x,y,t) = \pm\frac{\sqrt{-2a}}{2}$, where $\zeta = x + y \pm \frac{\sqrt{-2a}t^\alpha}{\alpha}$.

4. Graphical Illustration and Analysis

This section provides graphical depictions of the conformable fractional ZK equation to examine the influence of fractional order on the solutions of $\varphi_2(x,y,t)$, $\varphi_7(x,y,t)$, $\varphi_{11}(x,y,t)$ and $\varphi_{19}(x,y,t)$. The investigation is carried out by fixing the parameters $b = \nu = \zeta_0 = 1$ within the spatial-temporal region $0 \le x, t \le 5, y = 2$. The resulting three-dimensional (3D) plots corresponding to the fractional orders $\alpha = 1, 0.75, 0.5, 0.25$ are shown in panels (A)–(D), while panel (E) presents the corresponding two-dimensional (2D) projection with $\boldsymbol{x} = 1$.

Figure 1 displays 3D plots of the solutions of $\varphi_2(x,y,t)$ in panels (A-D) with parameters $\tau = -1, \rho = a = 1$. Panel (E) presents a 2D slice at $\boldsymbol{x} = 1$. The surface in panel A exhibits a steep, oscillatory wave pattern with a prominent crest near the origin. The amplitude remains high and the oscillations are well-defined, reflecting a strong nonlinear interaction between dispersion and nonlinearity. This indicates a classical soliton-like structure propagating in time without significant attenuation. In panel B, the amplitude of the wave slightly decreases and the oscillations become less pronounced. The wave still preserves its solitary character but with reduced intensity, suggesting partial energy loss due to the medium's memory characteristics. In panel C, the soliton shape becomes notably flatter, and the amplitude diminishes considerably. At panel D, the surface nearly flattens out, indicating minimal variation of the solution with respect to both space and time. The amplitude is very low, representing a highly dissipative regime. Panel E presents the two-dimensional projection of $\varphi_2(x,y,t)$ for different fractional orders. It clearly demonstrates that as α decreases, the amplitude of oscillation decays rapidly, and the peaks flatten.

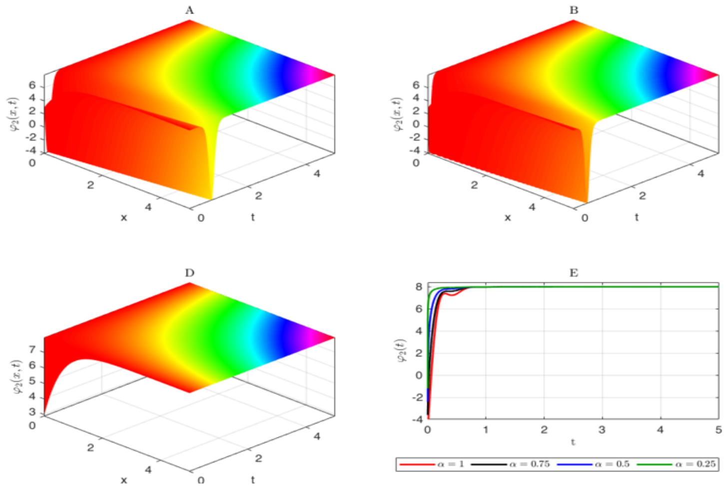

Figure 1. Graphical depiction of the nonlinear wave behavior of $\varphi_2(x,y,t)$, showing both 3D and 2D plots corresponding to several selected values of the parameter α.

Figure 2 (Panels A–D) illustrates the 3D evolution of the solutions $\varphi_7(x,y,t)$ for parameters, $\tau = -1, \rho = a = 1$, while Panel E shows a two-dimensional slice at $\boldsymbol{x} = 1$. In Panel A, a highly localized, sharp solitary peak appears near the origin, signifying strong nonlinearity with most of the system's energy concentrated at the crest. Panel B reveals multiple distinct peaks of varying amplitudes, indicating the formation of secondary solitary structures due to nonlinear interactions in the fractional framework. In Panel C, the main peak remains dominant but the distribution becomes irregular as fractional damping smooths the surrounding oscillations. Panel D represents a strongly dissipative case, where the surface flattens and the amplitude decreases significantly. Panel E demonstrates the temporal evolution of $\varphi_7(x,y,t)$ for different fractional orders, showing a clear reduction in amplitude as α decreases—transitioning from sharp, high-intensity peaks at α =1 to nearly constant, smooth profiles at α = 0.25

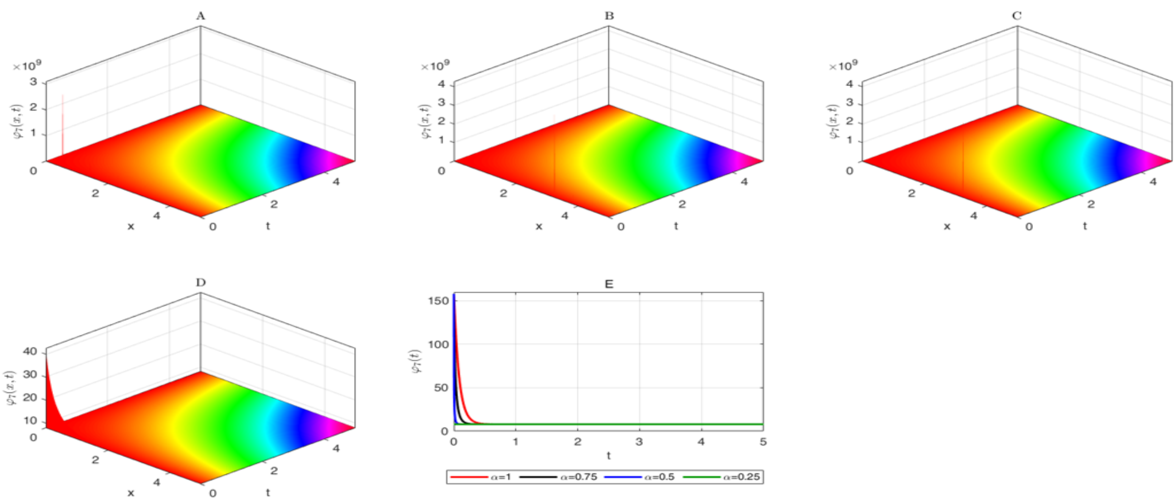

Figure 2. Graphical depiction of the nonlinear wave behavior of φ_7 *(x,y,t)*, showing both 3D and 2D plots corresponding to several selected values of the parameter α.

Figure 3 (Panels A–D) illustrates the 3D plots of the real part of solutions $\varphi_{11}(x,y,t)$ for parameters $\tau=\rho=a=1$, while Panel E shows a two-dimensional slice at $\boldsymbol{x}$ = 1. In Panel A, the surface demonstrates a highly periodic oscillatory structure with nearly constant amplitude, representing a stable nonlinear soliton state where dispersion and nonlinearity are balanced. When the fractional order decreases to α = 0.25 (Panel B), the oscillations become more irregular with sharper peaks, indicating stronger nonlinear interactions and partial energy redistribution. For α = 0.75 (Panel C), the amplitude begins to decay and the pattern smooths out as fractional damping dominates, signaling a shift toward a moderately dissipative regime. In the lowest case, α = 0.25 (Panel D), high-frequency oscillations with reduced amplitude emerge, showing the dominance of diffusion and the gradual loss of wave coherence. Panel E depicts the two-dimensional temporal evolution of $\varphi_{11}(x,y,t)$ across different fractional orders, confirming this transition from nonlinear oscillatory behavior to a diffusive state.

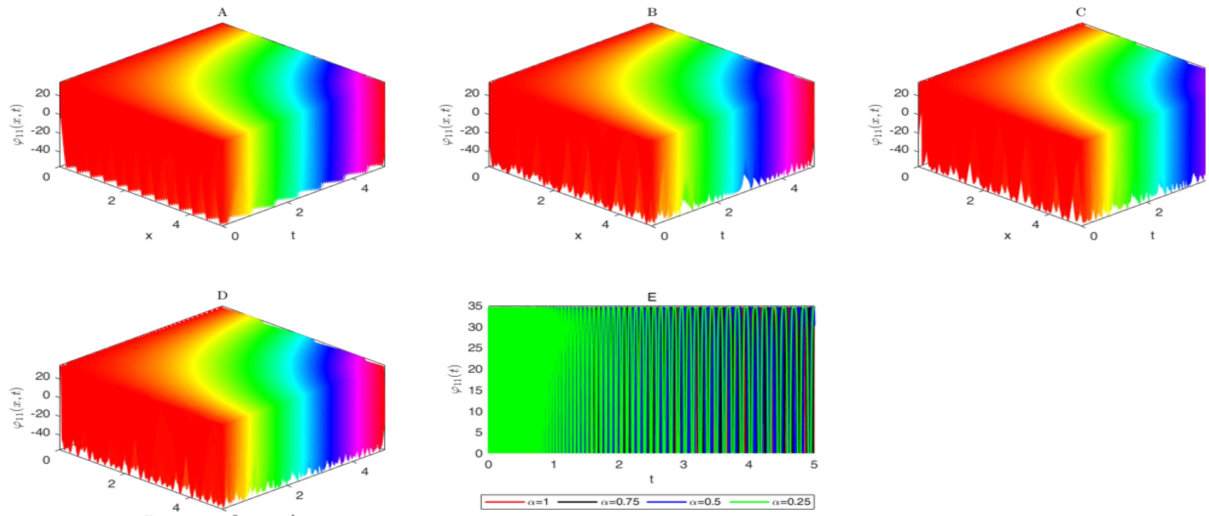

Figure 3. Graphical depiction of the nonlinear wave behavior of φ_{11} (x,y,t), showing both 3D and 2D plots corresponding to several selected values of the parameter α.

Figure 4 (Panels A–D) presents the three-*dimensional behavior of the solutions φ_{19} (x,y,t) for* parameters a = -1, ρ = 2, , while Panel E shows a two-dimensional slice at $\boldsymbol{x}$ = 1. In Panel A, a sharp and localized peak near the origin indicates a strong nonlinear solitary wave with most of the energy confined within a narrow region, representing a stable soliton formed by the balance between nonlinearity and dispersion. As shown in Panel B, the soliton amplitude decreases and the profile becomes smoother due to increasing dispersive and damping effects. In Panel C, the system enters a strongly dissipative regime where the amplitude drops sharply and the surface becomes nearly uniform, revealing the dominance of memory-driven diffusion over nonlinear effects. Panel E illustrates the temporal evolution of φ_{19} *(x,y,t)* at different fractional orders. The results indicate that as α decreases from 1.0 to 0.25, both the amplitude and intensity of the wave diminish progressively, transforming into a smooth and attenuated diffusive structure.

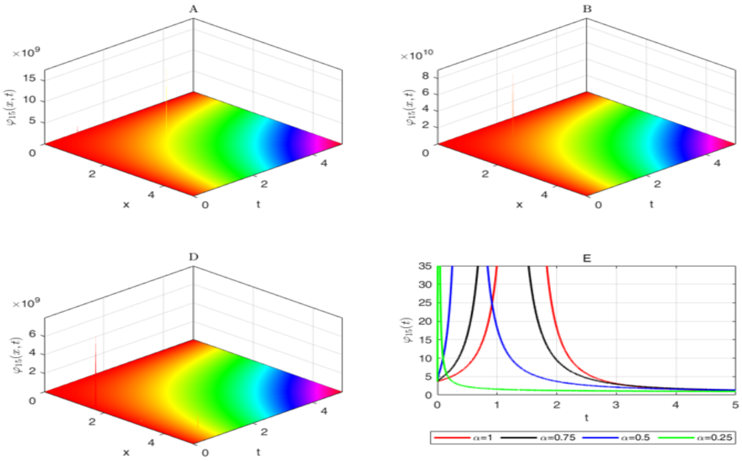

Figure 4. Graphical depiction of the nonlinear wave behavior of φ_{19} (x,y,t), showing both 3D and 2D plots corresponding to several selected values of the parameter α.

5. Stability Discussion

The stability of the traveling-wave solutions is examined by analyzing their response to small perturbations after reducing the conformable fractional -dimensional ZK equation to an ordinary differential equation through an appropriate traveling-wave transformation. The numerical simulations and graphical representations indicate that when the fractional order , the solutions preserve strongly localized, high-amplitude soliton structures, reflecting stable wave propagation arising from a balance between nonlinear and dispersive effects. As the fractional order decreases, increased damping and memory-related effects become dominant, resulting in gradual amplitude attenuation, smoother wave profiles, and the disappearance of secondary oscillatory features. Consequently, the system evolves toward more dissipative and asymptotically stable states. These observations are consistent with established stability results for KdV and ZK-type equations and demonstrate that the fractional parameter plays a crucial role in regulating stability, while the UM effectively captures the qualitative stability properties of the obtained solutions [22].

6. Conclusion

The present study applied the Unified Method to derive exact analytical solutions of the conformable fractional ZK equation. Multiple classes of nonlinear wave solutions were derived, illustrating how the fractional parameter influences amplitude, localization, and stability. The graphical results revealed that higher values of preserve strong soliton structures, while smaller values cause amplitude decay and enhanced diffusion, emphasizing the critical role of fractional derivatives in controlling nonlinear wave phenomena. The research demonstrates that the Unified Method provides a coherent, adaptable, and computationally efficient framework for solving fractional nonlinear partial differential equations. These results provide meaningful insight into the modeling of complex physical systems characterized by nonlocal and memory-dependent dynamics, and they establish a foundation for extending the proposed methodology to higher-dimensional and variable-coefficient fractional models. Further research may focus on the analysis of coupled nonlinear fractional systems as well as numerical investigations of the ZK equation.

7. References:

1. *Evans, L. C. (2010). Partial Differential Equations. American Mathematical Society.*
2. *Smoller, J. (1994). Shock Waves and Reaction-Diffusion Equations. Springer-Verlag. https://doi.org/10.1007/978-1-4612-0873-0*
3. *Gilbarg, D., & Trudinger, N. S. (2001). Elliptic Partial Differential Equations of Second Order. Springer-Verlag. https://doi.org/10.1007/978-3-642-61798-0*
4. *Wazwaz, A. (2009). Partial Differential Equations and Solitary Waves Theory. Higher Education Press / Springer-Verlag. https://doi.org/10.1007/978-3-642-00251-9*
5. *Welly, H. N. A. (1997). Symbolic method to construct exact solutions of nonlinear partial differential equations. Mathematics and Computers in Simulation, 43, 13–27. https://doi.org/10.1016/S0378-4754(96)00053-5*
6. *Dodd, R. K., Eilbeck, J. C., Gibbon, J. D., & Morris, H. C. (1982). Solitons and Nonlinear Wave Equations. Academic Press.*
7. *Chen, Y., & Wang, Q. (2005). Extended Jacobi elliptic function rational expansion method and abundant families of Jacobi elliptic function solutions to the (1 + 1)-dimensional dispersive long wave equation. Chaos, Solitons & Fractals, 24(3), 745–757. https://doi.org/10.1016/j.chaos.2004.09.014*
8. *Wang, M., Li, X., & Zhang, J. (2008). The (G'/G)-expansion method and travelling wave solutions of nonlinear evolution equations in mathematical physics. Physics Letters A, 372(4), 417–423. https://doi.org/10.1016/j.physleta.2007.07.051*
9. *Malfliet, W., & Hereman, W. (1996). The tanh method: Exact solutions of nonlinear evolution and wave equations. Physica Scripta, 54(6), 563–568. https://doi.org/10.1088/0031-8949/54/6/003*
10. *Li, W.-A., et al. (2009). The (w/g)-expansion method and its application to the Vakhnenko equation. Chinese Physics B, 18(2), 1–6. https://doi.org/10.1088/1674-1056/18/2/004*
11. *Hammouch, Z., & Mekkaoui, T. (2013). Approximate analytical solution to a time-fractional Zakharov–Kuznetsov equation. International Journal of Physical Research, 1(2), 28–33. https://doi.org/10.14419/ijpr.v1i2.849*
12. *G. Jumarie, Modified Riemann-Liouville derivative and fractional Taylor series of nondifferentiable functions further results, Computers & Mathematics with Applications, Volume 51, Issues 9–10, 2006, Pages 1367-1376, ISSN 0898-1221, https://doi.org/10.1016/j.camwa.2006.02.001*
13. *Atangana A and Goufo E F D 2014 Extension of matched asymptotic method to fractional boundary layers problems Math. Probl. Eng. Mathematical Problems in Engineering 1*
14. *https://doi.org/10.1155/2014/107535*
15. *Diethelm, K. (2010). The analysis of fractional differential equations: An application-oriented exposition using differential operators of Caputo type. Springer-Verlag. https://doi.org/10.1007/978-3-642-14574-2*
16. *Khalil, R., Al Horani, M., Yousef, A., & Sababheh, M. (2014). A new definition of fractional derivative. Journal of Computational and Applied Mathematics, 264, 65–70. https://doi.org/10.1016/j.cam.2014.01.002*
17. *Al-Zhour, Z., Al-Mutairi, N., Alrawajeh, F., & Alkhasawneh, R. (2021). New theoretical results and applications on conformable fractional natural transform. Ain Shams Engineering Journal, 12(2), 927–933. https://doi.org/10.1016/j.asej.2020.07.006*
18. *Fokas, A. S. (1997). A unified transform method for solving linear and certain nonlinear PDEs. Proceedings of the Royal Society A, 453(1962), 1411–1443. https://doi.org/10.1098/rspa.1997.0077*
19. *T. Aydemir, Traveling-wave solution of the Tzitzéica-type equations by using the unified method, Theor. Math. Phys. 216 (2023), 944–960. https://doi.org/10.1134/S0040577923070048*
20. *Akcagil, S., & Aydemir, T. (2018). A new application of the unified method. New Trends in Mathematical Sciences, 6(2), 185–199. https://doi.org/10.20852/ntmsci.2018.261*
21. *Alam, N., Ullah, M., Nofal, T., Ahmed, H. M., Ahmed, K., & Al-Nahhas, M. (2024). Novel dynamics of the fractional KFG equation through the unified and unified solver schemes with stability and metastability analysis. Nonlinear Engineering, 13, 20240034. https://doi.org/10.1515/nleng-2024-0034*
22. *Ullah, M. S., Abdeljabbar, A., Roshid, H. O., & Ali, M. Z. (2022). Application of the unified method to solve the Biswas–Arshed model. Results in Physics, 42, 105946. https://doi.org/10.1016/j.rinp.2022.105946*
23. *Bona, J. L., & Souganidis, P. E. (1988). Stability and instability of solitary waves of Korteweg–de Vries type. Proceedings of the Royal Society of London A, 411, 395–412.*
24. *https://doi.org/10.1098/rspa.1987.0073*